J. Fluid Mech. (1996), *vol.* 311, *pp.* 219–237

Inertial coating of a fibre

By ALAIN DE RYCK AND DAVID QUÉRÉ
Laboratoire de Physique de la Matière Condensée, Collège de France,
75231 Paris Cedex 05, France

(Received 3 February 1995 and in revised form 6 November 1995)

Fibres can be coated by passing them through a solution. At low velocity, the thickness of the entrained film is given by the Landau law. For liquids of low viscosity, we discuss the high-speed withdrawal regimes which are of technological interest. We focus on inertial effects and geometrical limitations. New experimental data are presented and discussed by using dimensional arguments. Finally, a classification is proposed.

1. Introduction

Just after they are made, fibres (glass fibres or polymeric ones) are coated with a liquid in order to prevent them from breaking in further operations. The process simply consists in pulling them through a bath of liquid, so that they come out coated with a layer of liquid (see figure 1). The velocity at which the fibres are pulled is generally high (of the order of 10 m s^{-1}). The question we address in this paper is the thickness of the entrained film: what are the parameters which determine the thickness and what is (or are) the entrainment law(s) as a function of these parameters?

The problem of dynamic coating has principally concerned three kinds of geometry: withdrawal of a vertical plate out of an infinite reservoir (Morey 1940; Landau & Levich 1942; Derjaguin 1943), withdrawal of a fibre (Goucher & Ward 1922), and emptying of a capillary tube (Bretherton 1961). A particular case of planar withdrawal is the making of soap films from a surfactant solution (Mysels, Shinoda & Frankel 1959; Lyklema, Scholten & Mysels 1960; Mysels & Cox 1962). We focus in this paper on fibre withdrawal. After a brief review of previous work (which concerns low-velocity regimes) and a presentation of our experimental set-up (§2), we present data which allow us to extend the description to situations where inertia must be considered. Three effects are successively discussed, in §§3, 4 and 5.

2. Visco-capillar entrainment of liquid: review and experiment

2.1. *Pioneering work: from Goucher & Ward to Landau & Levich*

The first paper on dynamic coating was published in 1922 where Goucher & Ward studied both plate and fibre coating. For small fibres (of radius b much smaller than the capillary length $\kappa^{-1} = (\gamma/\rho g)^{1/2}$, where γ is the surface tension of the liquid, ρ its specific mass and g the acceleration due to gravity), they noticed that the effect of gravity is negligible. The thickness e of the entrained film is determined by a balance between the viscous forces (favourable to the film) and the capillary forces (which tend to limit the thickness, since the fibre distorts the interface when drawn out). Thus they proposed to look for solutions of the form

$$e = bf(Ca), \tag{1}$$

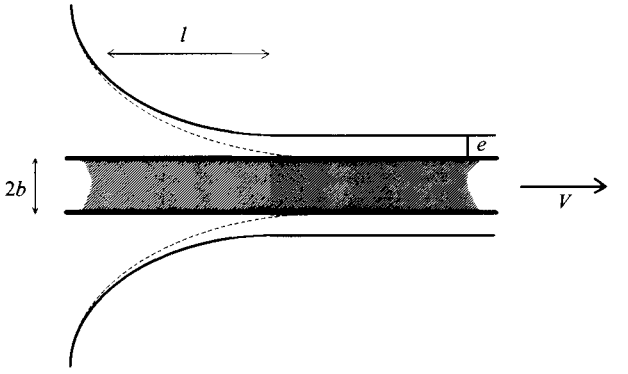

FIGURE 1. Withdrawal of a fibre out of a bath of wetting liquid. Because of the liquid entrainment, the static meniscus (dashed line) is strained for a length l.

where $Ca = \eta V/\gamma$ is the capillary number, η being the liquid viscosity and V the withdrawal velocity. Experimental data were obtained by coating metallic wires with melted beeswax and weighing them after solidification. They found that $f(Ca)$ is an increasing function close to linearity.

Twenty years later, Landau & Levich (1942) and Derjaguin (1943) proposed the first theory for the thickness of the film, for capillary numbers smaller than unity. Their description is based on figure 1. When pulling the fibre out of the bath, the static meniscus is deformed and a liquid film is entrained. As understood by Goucher & Ward, the thickness e of the film results from the competition between the viscous driving of the liquid by the solid and the capillary resistance of the surface to deformation.

The region where the film forms is called the dynamic meniscus, of thickness of order e and length l; l is determined by balancing the pressure between the static meniscus (of zero curvature if b is smaller than the capillary length) and the dynamic meniscus. The Laplace pressure in the latter incorporates two terms of opposite signs: one due to the curvature of the fibre and one related to the second derivative of the profile. Thus the balance between the two menisci dimensionally is

$$\frac{\gamma}{b+e} - \frac{\gamma e}{l^2} \sim 0. \tag{2}$$

For thin films ($e \ll b$), it leads to

$$l \sim (eb)^{1/2}. \tag{3}$$

In the (thin) film, the Laplace pressure is $\Delta p = \gamma/b$. Owing to this superpressure, a flow towards the reservoir takes place inside the dynamic meniscus. For small Reynolds numbers, this flow obeys the Poiseuille law

$$V \sim \frac{e^2}{\eta}\frac{\gamma}{lb}. \tag{4}$$

Eliminating l in (4) by using (3) yields

$$e \sim b(\eta V/\gamma)^{2/3}. \tag{5}$$

In their original paper, detailed calculations allowed Landau & Levich to calculate the numerical constant in (5). They found

$$e = 1.34bCa^{2/3}. \tag{6}$$

Equation (6) is sometimes referred to as the Bretherton law, since Bretherton showed that it also determines the thickness of the film left behind a drop inside a capillary tube, the difference being that b then represents the inner radius of the tube (Bretherton 1961).

2.2. *Reported deviations from the Landau & Levich law*

The role of gravity. For a fibre withdrawn vertically, the film also drains because of gravity. The gravity force can be neglected if it remains much smaller than the capillary suction, i.e. $\rho g \ll \gamma/(b+e)l$. For capillary numbers smaller than unity, this condition is ensured if

$$Bo \ll 1,$$

where Bo is the Bond number which compares capillary forces with gravity: $Bo = b^2/\kappa^{-2}$. The capillary length is generally of the order of a millimetre, so that the condition of small Bond number is satisfied if the fibre radius is smaller than typically 200 μm. The withdrawal of thick fibres (b of order κ^{-1}) has been investigated both theoretically (White & Tallmadge 1965) and experimentally (White & Tallmadge 1966).

For a fibre withdrawn horizontally, a Bond number much smaller than unity indicates that the film remains axisymmetric during the withdrawal (a necessary condition for establishing the Landau law).

Large capillary numbers. Equation (6) is only valid at small capillary numbers. When Ca tends to unity, e is no longer negligible compared with b. Then a simple correction, first proposed by White & Tallmadge (1966), consists in replacing b by $(b+e)$, so that the entrainment law (6) becomes

$$e = \frac{1.34bCa^{2/3}}{1-1.34Ca^{2/3}}. \tag{7}$$

This expression diverges for $Ca = 0.64$. At this point, the gradient of pressure between the film and the reservoir vanishes: in the absence of gravity, the reservoir is fully entrained by the fibre.

The role of surfactants. Carroll & Lucassen (1973) made oil films by pulling a textile fibre through an oil–water interface. The thickness was measured by dissolving the film in another oil and doing a titration of the mixture by gravimetry. They were mainly interested in the influence of surfactants on the film thickness. They predicted and observed (for Ca varying from 2×10^{-3} to 10^{-1}) that the presence of surfactants at the oil–water interface may thicken the film by a factor of order 2. Various attempts were made to explain this thickening. A recent discussion can be found for example in Ratulowski & Chang (1990).

Very small capillary numbers. Quéré, di Meglio & Brochard-Wyart (1989) were interested in the particular case of very slow withdrawal ($Ca < 10^{-6}$), out of a wetting liquid. When the film is thinner than the range of van der Waals forces (of order 100 nm), the disjoining pressure can thicken the film and the thickness becomes independent of the withdrawal velocity. Another cause of deviation at very small capillary number can be the surface roughness, as emphasized by Bretherton (1961) and shown by Chen (1986).

Non-wetting fluids. If the solid is slowly drawn out of bath of partially wetting liquid, it can come out dry (Sedev & Petrov 1992). Above a threshold in velocity (generally of order 1 cm s^{-1}), viscous forces dominate capillary ones, and a Landau regime is recovered (Quéré & Archer 1993).

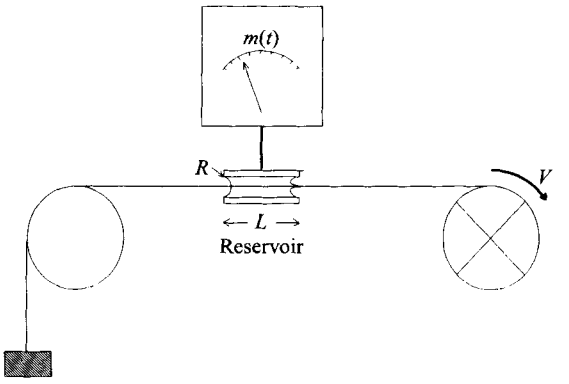

FIGURE 2. Sketch of the experimental set-up.

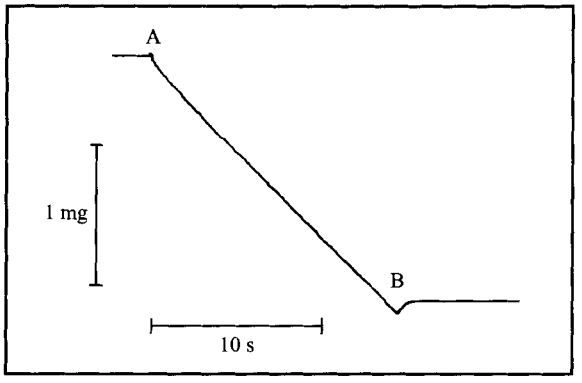

FIGURE 3. Mass of a drop of silicone oil of of viscosity $\eta = 19$ cP as a function of time. Between A and B, a nickel wire of radius $b = 63.5$ μm is drawn out of the drop at a velocity $V = 3$ cm s^{-1}. The mass decreases linearly with time, indicating that a film of constant thickness is entrained by the fibre. Solving equation (8) yields a film thickness of 7.8 μm.

2.3. *Principle of the experiment and first results*

To determine the thickness of the liquid layer coating a fibre, the experimental set-up sketched in figure 2 was devised. The idea is to measure the mass of the reservoir as time passes. The liquid bath is a drop trapped inside a horizontal Teflon tube of length L and radius R (if not specified: $L = 1.5$ cm and $R = 2$ mm). The fibre is pulled by a motor at the required velocity (measured by a tachometer) and passes through the tube. The fibre radius always remains much smaller and the reservoir aperture ($b \ll R$).

As soon as the fibre is moved, the mass m of the reservoir decreases since liquid is entrained by the fibre. An experimental recording is displayed in figure 3. The film thickness is deduced from such a plot by measuring the slope $\Delta m/\Delta t$ and solving the equation

$$e^2 + 2eb = \frac{-1}{\pi\rho V}\frac{\Delta m}{\Delta t}. \tag{8}$$

In the case of figure 3, the slope $\Delta m/\Delta t$ is a constant, which indicates that the film thickness is also a constant over time. The sensitivity of the measuring device means that the smallest thickness which can be measured by this method on a fibre of radius of order 50 μm is about 0.5 μm.

Because discrepancies observed by previous authors were imputed to the roughness

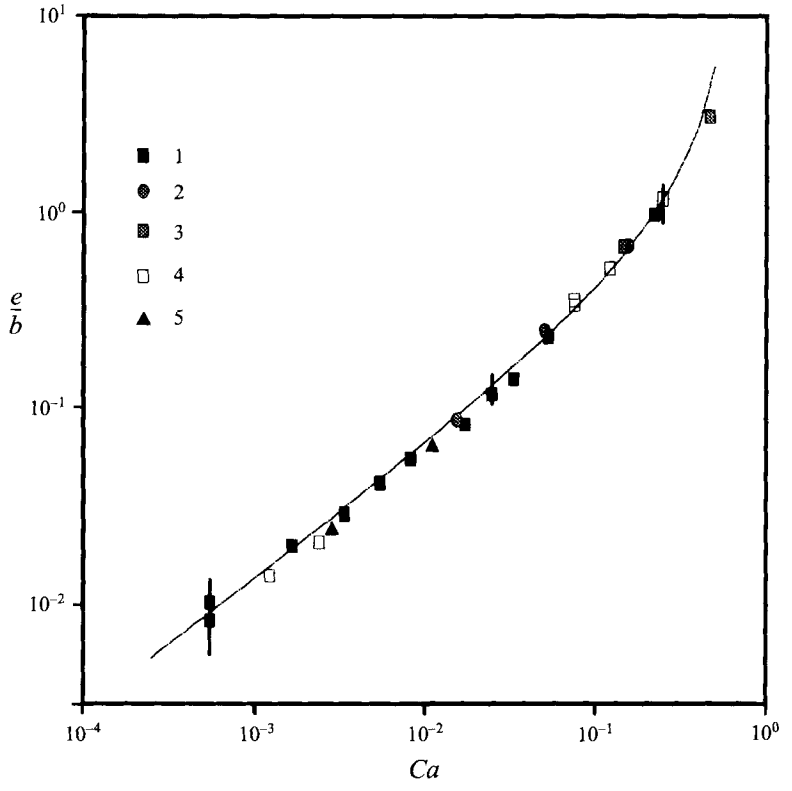

FIGURE 4. Dimensionless thickness e/b versus the capillary number $Ca = \eta V/\gamma$. Characteristics of the silicone oils used are: 1, $\eta = 19$ cP, $\gamma = 20.6$ dyn cm^{-1}; 2, $\eta = 96$ cP, $\gamma = 20.9$ dyn cm^{-1}; 3, $\eta = 291$ cP, $\gamma = 21.1$ dyn cm^{-1}; 4, $\eta = 485$ cP, $\gamma = 21.1$ dyn cm^{-1}; 5, $\eta = 12250$ cP, $\gamma = 21.1$ dyn cm^{-1}. The withdrawal velocities range from 150 μm s^{-1} to 5 cm s^{-1}. The fibre is a nickel wire of radius $b = 63.5$ μm, except for the point at the highest capillary number where it is a tungsten wire of radius $b = 12.5$ μm. The line repesents equation (7).

of the solids and to the presence of contaminants in the liquid, we chose to do the first series of experiments with smooth metallic wires and silicone oils (not sensitive to contamination, because of their low surface tension). The roughness of the fibres was estimated by AFM and SEM observations to be of order 200 nm (much lower than the film thicknesses).

In figure 4, the measured thickness divided by the fibre radius is presented as a function of the capillary number for different silicone oils. The characteristics of the oils are specified in the caption. The fibre is a nickel wire of radius $b = 63.5$ μm except for the point at the largest capillary number, obtained with a tungsten wire of radius $b = 12.5$ μm. The Bond numbers associated with these radii are respectively 2×10^{-3} and 7×10^{-5}. The withdrawal velocities range from 150 μm s^{-1} to 5 cm s^{-1}. The results are quite reproducible as indicated by the error bars displayed, except at the lowest capillary number where the limit of sensitivity of the mass measuring device is reached.

Equation (7) is drawn in the same plot, and fits quite well the experimental data over three orders of magnitude in capillary number. The agreement is good even for Ca approaching 0.64, because the thickness e remains smaller than both the radius R of the reservoir and the capillary length κ^{-1}. It was to satisfy these conditions that a smaller fibre was chosen for the point at largest Ca.

Thus for this model system (smooth fibres, viscous liquids of low surface tension and slow withdrawal), equation (7) is obeyed over a wide range of capillary numbers ($4 \times 10^{-3} < Ca < 0.5$). The film thickness results from a balance between the viscous forces, which are responsible for the film, and the capillary forces, which tend to make it as thin as possible. Therefore, we call this regime *visco-capillar*. It should describe the fibre coating at capillary and Reynolds numbers smaller than unity for all wetting fluids.

But in most practical applications, coating velocities are much higher and coating liquids are generally aqueous solutions instead of heavy oils. Thus we were interested in doing the same experiment at higher velocity with liquids of low viscosity (light silicone oil, pure water or water containing surfactants).

3. The visco-inertial regime

3.1. *Experimental results*

When doing the experiment described in §2.3 with liquids of low viscosity, the capillary number can remain small even if the velocity is high (with pure water for example, a withdrawal velocity of 70 cm s^{-1} corresponds to a capillary number of 0.01). Thus the data lie in the same interval of Ca as in §2.3 and can be directly compared with the results for oil. To reach higher velocities, the motor was changed. Three series of experiments were done: one with a light silicone oil (hexamethyldisiloxane of viscosity $\eta = 0.48$ cP, surface tension $\gamma = 15.9$ dyn cm^{-1} and specific mass $\rho = 0.76$ g cm^{-3}), one with pure water ($\eta = 1$ cP and $\gamma = 72.8$ dyn cm^{-1}) and the last one with two aqueous solutions of surfactant (in both cases: $\eta = 1$ cP and $\gamma = 37$ dyn cm^{-1}). Results with pure water were previously published for another fibre radius, showing the same effects as below (de Ryck & Quéré 1994).

Pure fluids. In figure 5, the film thickness is plotted versus the capillary number for the light silicone oil and for pure water. The fibre is a nickel wire of radius $b = 63.5$ μm, giving respective Bond numbers 2×10^{-3} and 5×10^{-4} (both much smaller than unity). The withdrawal velocity ranges from 20 to 76 cm s^{-1} for the oil and from 30 to 180 cm s^{-1} for water. In the same figure, the Landau law (6) is drawn and compared with the data.

For both liquids, the film thickness can be fitted by the Landau equation only at low velocity. Above a threshold Ca^*, a serious discrepancy can be observed. The film thickness sharply rises with the capillary number: it increases about tenfold by simply doubling the velocity. A diverging behaviour was also encountered with viscous oils, but it was very different: in figure 4, it can be seen that the divergence was much smoother, and occurred at a capillary number of order 1, instead of 0.01 with pure water. Thus this effect is a new one and seems to be linked to the low viscosity of the fluids.

Surfactant solutions. The same experiment was done with two aqueous solutions of sodium dodecyl sulphate (SDS) of concentration 20 g l^{-1} (about eight times the critical micellar concentration, or c.m.c.) and 2.4 g l^{-1} (the c.m.c.). The fibre is also a nickel wire of radius $b = 63.5$ μm (so that the Bond number is 10^{-3}). The results are displayed in figure 6 and again compared with equation (6). As for pure liquids, two successive types of behaviour can be observed.

At low capillary number ($Ca < Ca^*$), the entrainment law is slightly different from a Landau regime: the film is thicker than predicted by a factor of order 2. As mentioned above, this effect was previously reported by Carroll & Lucassen (1973), and by ourselves (de Ryck & Quéré 1993*a*). The thickening is due to the presence of

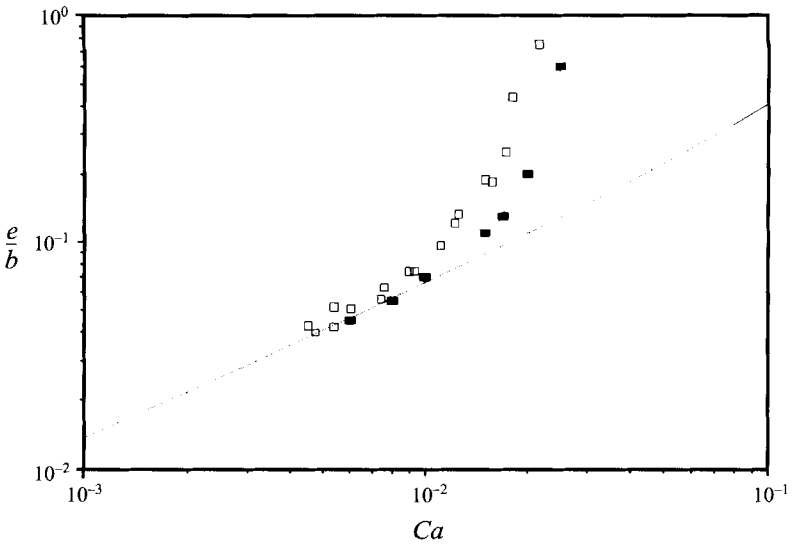

FIGURE 5. Dimensionless thickness of films entrained by a nickel wire of radius $b = 63.5$ μm withdrawn from pure water ($\gamma = 72.8$ dyn cm^{-1} and $\eta = 1$ cP; open squares) and from hexamethyldisiloxane ($\gamma = 15.9$ dyn cm^{-1} and $\eta = 0.48$ cP; black squares) versus the capillary number. The dashed line represents (7).

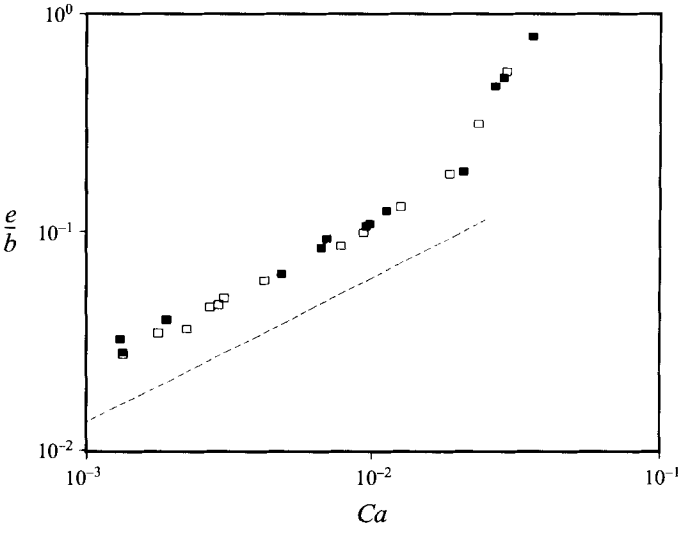

FIGURE 6. Film thickness divided by the fibre radius ($b = 63.5$ μm) versus the capillary number for a nickel wire drawn out of a SDS solution of concentration 2.4 g l^{-1} (black squares) or 20 g l^{-1} (open squares). The dashed line is the Landau law (6).

surfactants. Because of the fibre movement, a gradient of surfactant concentration is generated in the dynamic meniscus. It induces a Marangoni flow from the region of low surface tension (the reservoir) to the region of high surface tension (the film), so that the film gets thicker. An important feature related to this effect is that the thickening factor cannot exceed 2.5 (Ratulowski & Chang 1990), and thus is much lower than observed in the 'diverging' part of the curve.

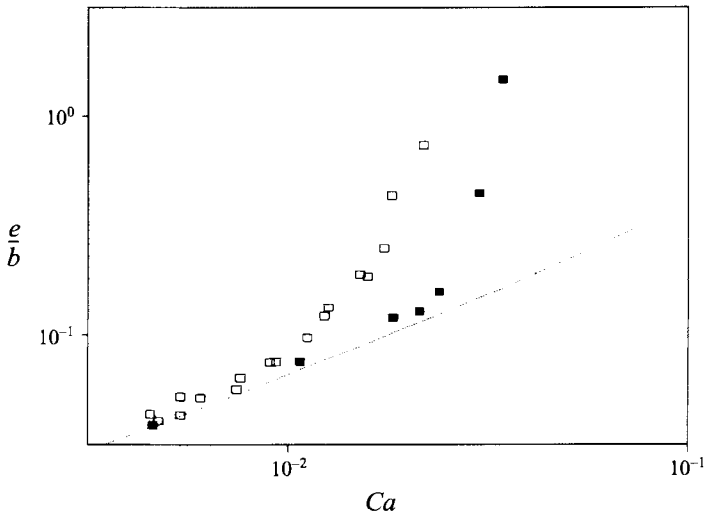

FIGURE 7. Dimensionless film thickness versus the capillary number. The films are drawn from pure water by a nickel wire of radius $b = 63.5$ μm (open squares) or by a tungsten wire of radius $b = 12.5$ μm (black squares). The dashed line represents (7).

The second regime in figure 6 concerns higher capillary numbers ($Ca > Ca^*$) and is similar to the one observed with pure liquids: above Ca^*, the film thickness sharply rises. The threshold is the same for both surfactant solutions, and is slightly shifted towards a smaller capillary number when compared with that observed for pure water.

Effect of the radius. The way the threshold depends on the fibre radius was also studied. In figure 7, the film thickness for pure water is plotted versus Ca for two different radii. The first fibre is the nickel wire previously used ($b = 63.5$ μm) while the second one is a molybdenum wire about five times thinner ($b = 12.5$ μm). It can be seen that doing the same experiment with a much thinner fibre makes the threshold shift towards higher capillary numbers: Ca^* roughly doubles for the thin fibre.

3.2. *The Weber number*

The increase in film thickness happens when doing experiments at high velocity. Moreover, it occurs even if the liquid contains surfactants, indicating that it is not a surface effect. Thus inertia was suspected to be responsible for this effect.

The reason why inertia sharply thickens the film can be understood as follows. The liquid enters the dynamic meniscus at a velocity of order V, and there undergoes a gradient of Laplace pressure. If the kinetic energy of fluid (per unit volume) is larger than the capillary pressure, the latter can be neglected and nothing retains the liquid any longer: the thickness diverges. It is logical to introduce the Weber number W as a parameter measuring the importance of inertia. W is defined by comparing the dynamic pressure (of order ρV^2) with the Laplace pressure (of order γ/b when $e \ll b$) (Epikhin & Shkadow 1978):

$$W = \frac{\rho V^2 b}{\gamma}.$$

Values of W associated with the experiments can be calculated. In the previous section (visco-capillar entrainment), the maximum velocity was 5 cm s^{-1} and so W was smaller than 0.01: inertia could indeed be neglected, a condition for satisfying the Landau

equation. For the experiments reported in this section, the situation is quite different. In figure 5, the divergence occurs at around 80 cm s^{-1} for the silicone oil and around 140 cm s^{-1} for water, which gives W of 1.9 and 1.7 respectively; similarly, we get for soapy water (figure 6) 115 cm s^{-1} and for the thin fibre (figure 7) 260 cm s^{-1} giving W of 2.3 and 1.2 respectively. These values are indicative, since the location of the divergence is rather inaccurate, but all are found to be of order unity. Similarly the value of W at the threshold of the thickness increase can be deduced from the data: in all the cases, W is found to be of order 0.1 there. Thus the discrepancy observed in figures 5–7 can be attributed to inertia. We call the anomalous behaviour above the Ca^* the *visco-inertial regime.*

3.3. *Shape of the divergence: a dimensional analysis*

The scaling laws associated with the visco-inertial behaviour can finally be specified. The dimensional Navier–Stokes equation is

$$\frac{\rho V^2}{l} \sim \frac{\gamma}{lb} + \frac{\eta V}{e^2}, \tag{9}$$

where l is the length of the dynamic meniscus. The signs in (9) must be stressed: most of the liquid entrained in the reservoir by viscosity bumps into the free surface, so that the Laplace pressure gradient and the convective term have opposite effects. Equation (9) can be rewritten in the form

$$\eta V \sim \frac{e^2}{l}\left(\frac{\gamma}{b} - \rho V^2\right) \tag{10}$$

which looks like (4), if an effective pressure is taken as $p = \gamma/b - \rho V^2$; l has still to be estimated. Using the same kind of arguments as in establishing (2) but taking into account inertia, we get (supposing $e \ll b$)

$$\frac{\gamma}{b} - \frac{\gamma e}{l^2} \sim \rho V^2. \tag{11}$$

Combining (10) and (11) yields an expression for the thickness:

$$e \sim \frac{bCa^{2/3}}{1 - W}, \tag{12}$$

where the role of the Weber number is clearly emphasized. If W is small (i.e. at small velocity), (12) reduces to (6). As W reaches unity, the thickness diverges: the Laplace pressure is not efficient enough to oppose to the inertia of the fluid drawn by the fibre coming out of the reservoir. The finite velocity V^* at which the film thickness diverges is dimensionally given by taking $W = 1$:

$$V^* \sim \left(\frac{\gamma}{\rho b}\right)^{1/2}. \tag{13}$$

Taking typical values for the different parameters ($\gamma = 30$ dyn cm^{-1}, $\rho = 1$ g cm^{-3} and $b = 50$ μm) leads to V^* of order 1 m s^{-1}, in agreement with the values observed experimentally. Moreover, the dimensional form of V^* explains why it slightly depends on the nature of liquid (see figures 5 and 6). For example, Ca^* varies as $1/\gamma^{1/2}$, which

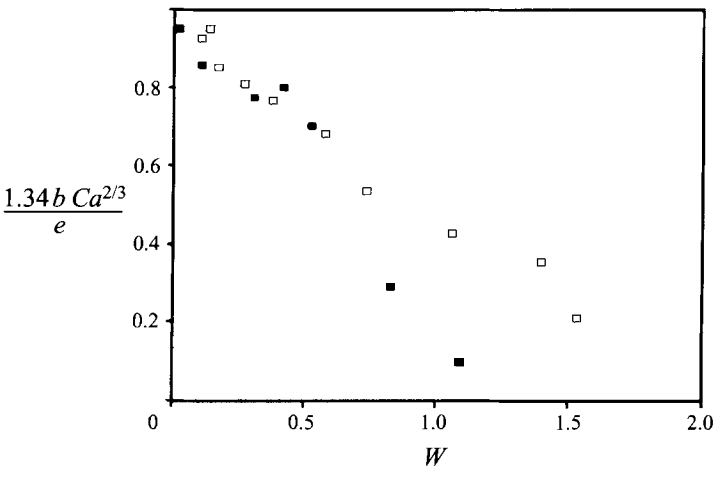

FIGURE 8. Landau thickness (6) or (7) divided by the experimental thickness versus the Weber W, for the data of figure 7 (open squares: $b = 63.5$ μm; black squares: $b = 12.5$ μm). The Weber number W is defined by comparing the kinetic energy per unit volume of the liquid with the Laplace pressure in the film ($W = \rho V^2 b/\gamma$).

is consistent with the observation of a larger Ca^* for the surfactant solution than for pure water. Also, the dependence on the fibre radius is predicted by (13) (Ca^* varies as $1/b^{1/2}$), in good qualitative agreement with the experimental behaviour in figure 7.

The shape of the divergence law (12) can be compared with the data. In figure 8, the Landau thickness divided by the experimental one (corresponding to the data of figure 7) is plotted as a function of W instead of Ca. Decreasing lines are obtained, in rough agreement with (12): they intersect the x-axis around $W = 1$ and the y-axis around 1, as expected. Dispersion at large thickness mainly comes from the fact that for large e, b should be replaced by $(b+e)$ in the definition of the Weber number.

It must be finally noticed that the visco-inertial divergence should be observed only if it occurs at a capillary number smaller than 1, the value for which a smooth capillary divergence takes place (as seen above, in (7) and figure 4). Together with (13), it gives a condition for observing this regime. Written for example in terms of the viscosity, it reads

$$\eta < (\gamma\rho b)^{1/2}.$$

For typical values (given above), it implies a viscosity smaller than 40 cP (a condition fulfilled in this section and in most practical situations).

3.4. *Conclusion*

In spite of its approximate nature, the dimensional analysis gives a physical understanding of the visco-inertial regime in satisfactory agreement with the data. Of course, it must be complemented by more detailed calculations. Following Esmail & Hummel (1975) who first tried to incorporate inertia in the Landau problem of plate coating, several attempts were recently published (de Ryck & Quéré 1993*b*; Koulago *et al.* 1995) or are under current study (V. Shkadov & A. Koulago 1995, personal communication). Analytical expressions or numerical results were obtained, in good agreement with the data. The diverging behaviour was found, and shown to be specific to the fibre geometry. In the plate geometry, effects of inertia are much less spectacular (Soroka & Tallmadge 1971; Esmail & Hummel 1975) since they are dominated by

gravity. A small divergence should also exist (de Ryck & Quéré 1995) but reduced by gravity which makes the liquid flow down, and thus limits the thickness.

The way the diverging regime ends has not yet been presented: we are now interested in what happens at still higher withdrawal velocities, which are closer to the industrial conditions of lubrication of polymeric and glass fibres where coating velocities are of order 10 m s^{-1}.

4. The boundary layer regime

For liquids of low viscosity, we have seen in the previous section that the film thickness diverges, at a capillary number of order 0.01 for aqueous solutions. At first sight, a natural limitation for the divergence is the aperture of the reservoir (namely the radius R of the tube). Looking for an eventual saturation of the thickness, a much more interesting (i.e. more general) behaviour was found.

4.1. *The viscous boundary layer*

When the fibre passes through the reservoir, the surrounding liquid close to the fibre starts to move because of the liquid viscosity. The layer entrained is the so-called viscous boundary layer. Its thickness δ grows dimensionally as $(\nu t)^{1/2}$, where t is the contact time between the solid and the liquid and ν the kinematic viscosity ($\nu = \eta/\rho$). So at the exit of the reservoir, the thickness of the boundary layer is

$$\delta \sim \left(\frac{\eta L}{\rho V}\right)^{1/2}, \tag{14}$$

where L is the length of the reservoir. At low velocity, δ is large compared with the thickness of the entrained film, given by (6), (7) or even (12), and the arguments proposed in §3 can be used. But at high velocity, the boundary layer becomes thinner than the film thickness predicted by (12). Then, the quantity of liquid entrained by the solid is expected to be given by the flux of liquid due to the fibre displacement inside the reservoir. Hence only the viscous boundary layer goes with the fibre ($e \sim \delta$) and the thickness is simply given by

$$e = \alpha\left(\frac{\eta L}{\rho V}\right)^{1/2}, \tag{15}$$

where α is a numerical coefficient. To check this expression, two different experiments were done.

4.2. *Emptying of the reservoir*

We let the reservoir be emptied by the fibre passing through it. As the length $L(t)$ of the reservoir decreases, the boundary layer gets thinner as time passes. But now, the film thickness should depend on L and vary as $L(t)^{1/2}$ (equation (15)). In figure 9, the mass of the reservoir is plotted versus time for a nylon fibre of radius $b = 110$ μm withdrawn at $V = 1.6$ m s^{-1} out of a reservoir of water (radius $R = 2$ mm and initial length $L_0 = 5.1$ cm). These parameters have been chosen to give a viscous boundary layer thinner than the film thickness calculated by (12): the fibre is rather thick so that the divergence threshold is less than 1 m s^{-1}. Thus the velocity is far in excess of V^*, inside a purely inertial regime: the corresponding Weber number is 6.

The new fact is that the curve $m(t)$ is no longer linear (as it was in figure 3) but, rather, looks like a parabola. This is in agreement with the arguments given above: as time passes, the reservoir gets shorter and the film thinner. Supposing that e is given

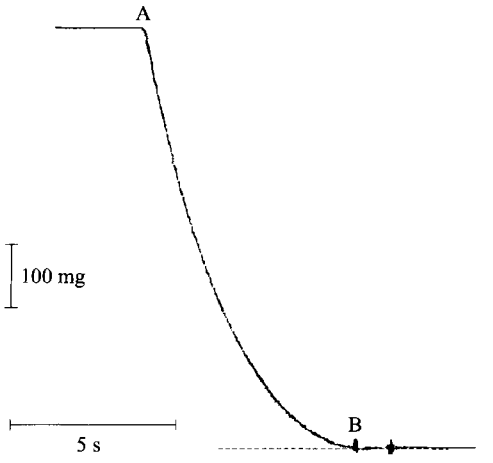

FIGURE 9. Mass of the reservoir as a function of time. A: the motor is switched on and a nylon fibre ($b = 110$ μm) is drawn out of pure water at a velocity $V = 1.6$ m s^{-1}. B: the reservoir is empty.

by (15), we have: $e \sim L^{1/2}$. Also, when the film is very thin (at the end of the experiment, close to the apex of the supposed parabola), we have $e \ll b$ and thus by (8) $\mathrm{d}L/\mathrm{d}t \sim -e$ since the mass of the drop is simply proportional to its length. These two conditions quickly give $L \sim t^2$, in agreement with figure 9.

A precise fit of the experimental curve $m(t)$ with that calculated assuming that the film thickness follows (15) can be done. As the tube is totally dried by the fibre (Teflon is not wetted by water so that there is no film remaining in the tube when the drop shortens), the mass is simply proportional to the length:

$$m(t) = \rho\pi R^2 L(t).$$

The loss of mass of the reservoir is given by (8). Supposing that the thickness is given by (15), equation (8) can be rewritten as a differential equation for the length of the drop:

$$-\frac{\mathrm{d}L}{\mathrm{d}t}R^2 = \left(\frac{\alpha^2\eta}{\rho}L + 2\alpha b\left(\frac{\eta V}{\rho}\right)^{1/2}L^{1/2}\right). \tag{16}$$

Setting $$\tau = \frac{2\rho}{\eta}\left(\frac{R}{\alpha}\right)^2 \quad \text{and} \quad \zeta = 2 + \left(\frac{\eta\alpha^2 L}{\rho V b^2}\right)^{1/2},$$

equation (16) reduces to a simple linear equation:

$$-\frac{\mathrm{d}\zeta}{\mathrm{d}t} = \frac{\zeta}{\tau} \tag{17}$$

which can be easily solved. The length of the drop is obtained as a function of time:

$$L(t) = \frac{4\rho V b^2}{\eta\alpha^2}\left[\exp\left(\frac{\eta\alpha^2}{2\rho R^2}t\right) - 1\right]^2, \tag{18}$$

where the origin of time is chosen at the moment when the drop has disappeared

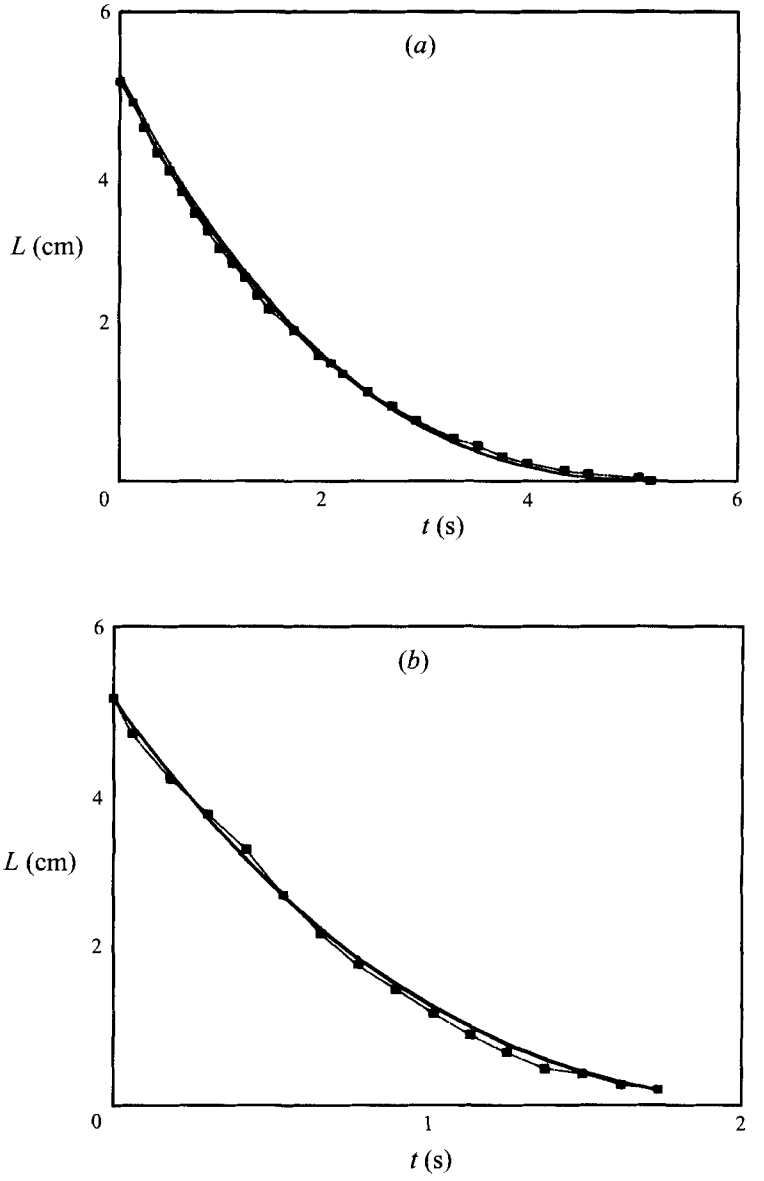

FIGURE 10. Length of a reservoir of pure water as a function of time. The reservoir is emptied by a nylon fibre of radius $b = 110$ μm. The black squares are the experimental data, and the line is the best fit with (18), giving a determination for the numerical constant α in (15). The fibre is withdrawn (*a*) at a velocity $V = 1.9$ m s^{-1} giving $\alpha = 0.9$ and (*b*) at $V = 4.8$ m s^{-1}, giving $\alpha = 1.3$.

($L(0) = 0$). Expanding (18) at short time gives the parabolic dependence which was mentioned above: $L(t) = (\alpha^2 \eta V b^2 / \rho R^4)\, t^2$.

Equation (18) fits the experimental curves quite well as can be seen in figure 10. Moreover, the fit allows us to determine the coefficient α. In figure 11, α is plotted as a function of the velocity, for V ranging from 1.6 to 4.8 m s^{-1}. The coefficient α is close to unity. It depends slightly on the velocity in the transition regime (where the thickness passes from the visco-inertial behaviour (equation (12)) to the boundary layer regime (15), but becomes constant at large velocity: then, we get $\alpha = 1.3 \pm 0.1$. This value may

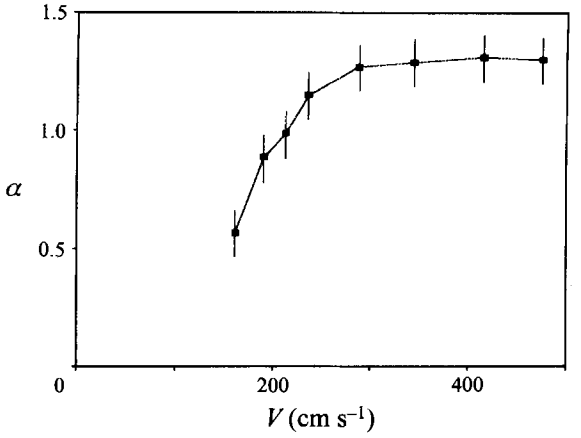

FIGURE 11. Value of coefficient α as a function of the withdrawal velocity. α is determined as indicated in figure 10. All the experiments are done with a nylon fibre of radius $b = 110$ μm drawn out of pure water.

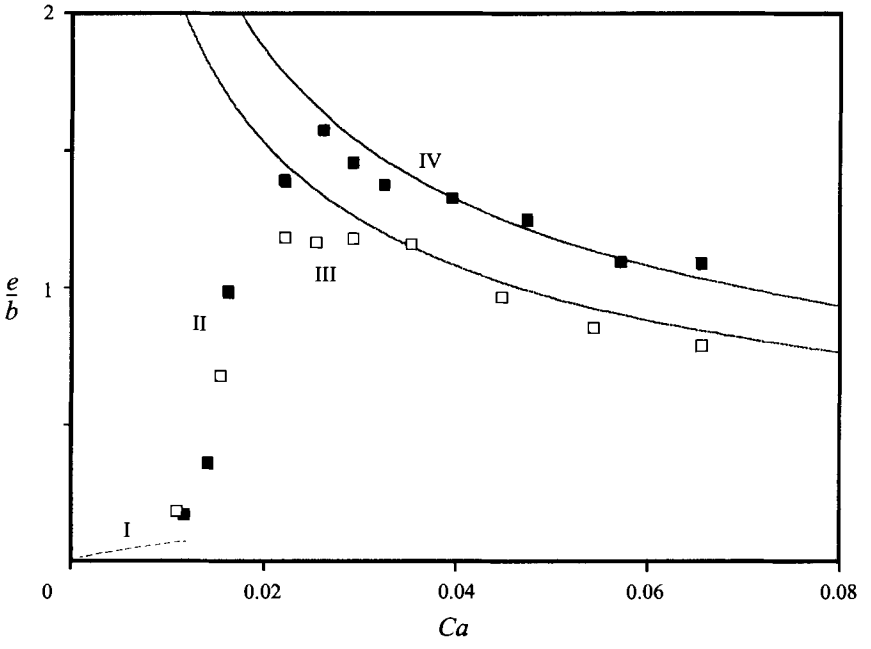

FIGURE 12. Dimensionless thickness versus the capillary number, at a fixed reservoir length $L_0 = 3.5$ cm (open squares) or $L_0 = 5.1$ cm (black squares). The experiments are done with a nylon fibre of radius $b = 110$ μm drawn out of pure water.

be compared with the one theoretically obtained in the case of a semi-space entrained by a plane. The flux (per unit width) is $Q \approx 1.7V(vt)^{1/2}$ (Landau & Lifshitz 1959), which gives α of about 1.7.

4.3. *Thickness as a function of the velocity*

In the boundary layer regime, the film thickness for a fixed drop length is expected to decrease with the velocity, as $1/V^{1/2}$. In figure 12, the reduced thickness e/b has been plotted versus Ca. It corresponds to experiments done with a nylon fibre of radius

$b = 110$ μm drawn out of pure water with two different initial lengths for the reservoir: $L_0 = 3.4$ cm and 5.1 cm. The coating velocity ranges between 70 and 5 m s^{-1} (so that W varies from 1 to 40). For a given velocity, plots similar to figure 11 were obtained. The film thickness at a fixed reservoir length is simply deduced from the measurement of the slope dm/dt at the required length.

Finally figure 12 summarizes all the regimes successively encountered: (i) in region I, the dashed line represents the Landau law (6); (ii) region II is the visco-inertial divergence described in §3; (iii) region III is the transition between the visco-inertial regime and the boundary layer regime. In this small region, the thickness roughly follows (15), but with a slight dependence of the coefficient α on V; (iv) finally, the graph gives prominence to the velocity dependence in the boundary layer regime (region IV). The two solid curves obey (15), with $\alpha = 1.1$ for the two lengths employed. The numerical constant used for these fits is slightly smaller than above (where it was shown to tend to 1.3) but the way it is determined is less precise here.

While the boundary layer regime seems to be established and qualitatively understood, detailed calculations remain to be done to predict the value of the coefficient α and the way it depends on the velocity in the transition regime.

5. The particular case of long reservoirs

We finally tried to investigate the transition regime between the divergence and the viscous boundary layer regime. A naive idea consisted in replacing the short reservoir (length of order 1 cm) by a much longer one (length of order 10 cm), so that the viscous boundary layer had more time to develop, even at large withdrawal velocities. But doing this led to unexpected results.

The reservoir is still a Teflon tube (radius $R = 2$ mm) but much longer: $L_0 = 30$ cm. It is filled with pure water and emptied by making a nickel wire of radius $b = 88.5$ μm pass through it. Because of the bigger mass associated with the new length, the mass measuring device is changed.

Direct observations reveal a new phenomenon. At low velocity ($Ca \ll Ca^*$), nothing special happens and the Landau regime is followed. But if the velocity becomes larger than 50 cm s^{-1}, the meniscus at the exit of the reservoir tube breaks and drops are expelled. Hence the recorded curve $m(t)$ has a step shape, as shown in figure 13. Each step corresponds to the expulsion of a drop of radius r. The step height gives $r = 2.2$ mm, (logically) showing that r is of order R, the aperture of the reservoir. Between two steps, the mass is not a constant but slowly decreases: the fibre entrains a film of thickness obeying (12).

In this case, it is no longer possible to get an $e(V)$ curve from the weight experiment, because the fluid is removed both as a drop and as a film. Nevertheless, an 'effective thickness' is reported in figure 14, corresponding to the average flux $\Delta m/t$ at the beginning of the experiment ($L = L_0 = 30$ cm). These data are compared with those obtained with $L_0 = 10$ cm, for which such a drop-expelling behaviour was not observed. The line in the graph represents (15) with $\alpha = 1.3$, which shows that when drops are expelled, the time-averaged flux is close to the boundary layer flux.

Interpretation. The capillary force f_γ retaining the meniscus and anchoring the drop inside the horizontal tube is of order

$$f_\gamma \sim \gamma R. \tag{19}$$

The fluid set in motion by the fibre exerts a force f_η on the meniscus which can be

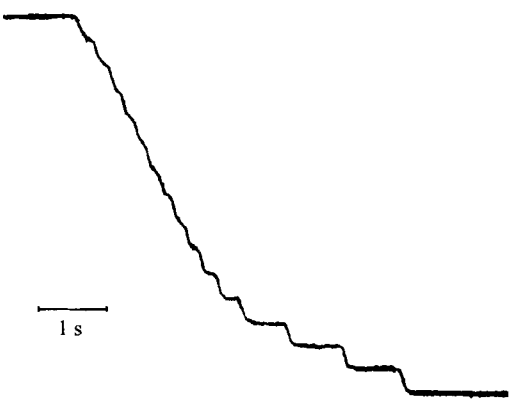

FIGURE 13. Mass of a very long reservoir ($L_0 = 30$ cm) filled with water as a function of time. The reservoir is emptied by a nickel wire ($b = 88.5$ μm) pulled at $V = 50$ cm s^{-1}.

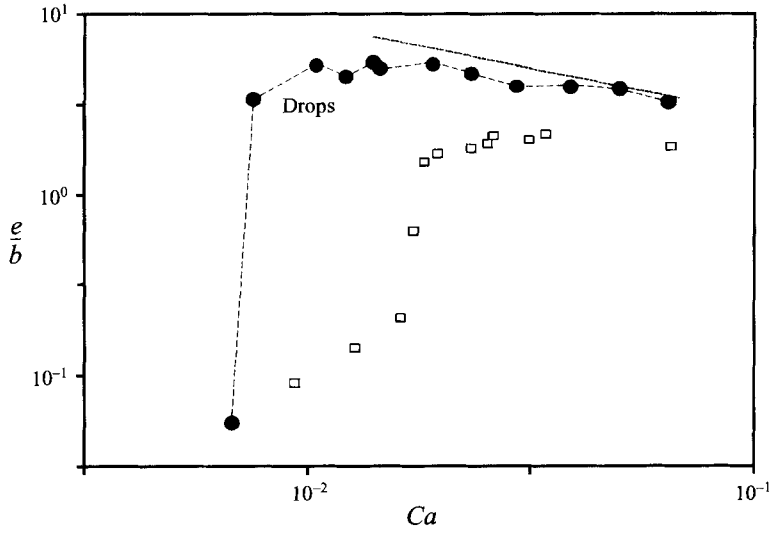

FIGURE 14. Dimensionless effective thickness (defined in the text) versus the capillary number. The fibre is a nickel wire ($b = 88.5$ μm) pulled out of pure water, for two different reservoir lengths: $L_0 = 10$ cm (squares) or $L_0 = 30$ cm (circles). The dotted line corresponds to the viscous boundary regime.

written as a dynamic pressure (of order ρV^2) times the area on which it acts, of order δ^2 (L is large and we have $\delta \gg b$). δ is given by (14), which yields

$$f_\eta \sim \eta V L. \tag{20}$$

If f_η exceeds the capillary force, the meniscus twists (like an umbrella in the wind) and a drop is removed. By setting f_γ and f_η to be equal, a criterion for the appearance of the drop regime is obtained:

$$LCa \sim R. \tag{21}$$

For $R = 2$ mm and $L = 30$ cm, (21) gives as a threshold $Ca = 0.007$ (or $\log Ca = -2.2$), close to the experimental value observed in figure 14.

For a given velocity V and aperture R, drop expulsion occurs if the reservoir is long enough, i.e. if its length is larger than $L^* = RCa^{-1}$. If a long reservoir ($L_0 > L^*$) is emptied by drawing a fibre out of it, drops are first expelled but the drop regime stops

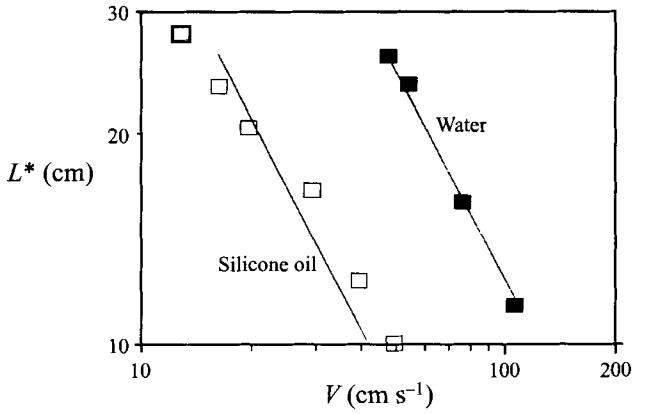

FIGURE 15. Critical length L^* versus the velocity V, measured for water (black squares) and for hexamethyldisiloxane (open squares). The continuous lines correspond to (21).

when $L(t)$ reaches L^*, which can thus be directly observed. In this way, L^* was determined as a function of the velocity for two different liquids: pure water and the light silicone oil described above ($\gamma = 15.9$ dyn cm^{-1} and $\eta = 0.48$ cP). The results displayed in figure 15 show a quite good agreement with equation (21), though all the numerical coefficients have been neglected.

6. Conclusion

Different experiments on fibre coating have been presented. First, slow coating (corresponding to negligible Weber numbers) of thin smooth fibres by viscous oils was shown to obey the well-known Landau equation (6). This regime was referred to as *visco-capillar*, since the film thickness results from a balance between capillarity and viscosity. The special case of extremely slow coating, where long range forces must be taken into account, was not considered here.

Then we were interested in describing coating by liquids of low viscosity (such as water) at higher velocity (about 1 m s^{-1}). The measurements were shown to deviate tremendously from the Landau law, even if the capillary number remained negligible compared with unity ($Ca < 0.05$). Two successive regimes were found and discussed. First the film thickness sharply increases around a critical velocity V^*, and then slowly decreases for V much larger than V^*.

This diverging behaviour was shown to happen as the Weber number becomes of order 1. it is due to inertia and thus this was called *visco-inertial regime*. A dimensional form for the critical velocity V^* was proposed and studied. At larger velocities ($W > 1$), the fibre entrains just the viscous boundary layer and the film thickness decreases as $1/V^{1/2}$. It does not depend any longer on the surface tension but is limited by the geometry of the reservoir since it is fixed by the length of the bath. Practically this *boundary layer regime* should be relevant to most industrial coating processes, where fibres are lubricated with aqueous solutions at a velocity of order 10 to 100 m s^{-1}.

The special case of very long reservoirs was finally discussed. A third inertial effect was found: at high velocity, a new regime appears, where drops of liquids are regularly expelled from the bath. This instability of the meniscus was studied by taking into account the dynamic pressure exerted on it. A simple criterion for the appearance of the instability was proposed.

For all the effects, dimensional analysis was done in order to explain physically the observations. Scaling laws were obtained, emphasizing the parameters which control the phenomena and allowing us to propose a simple classification. Detailed calculations remain to be done to get fully quantitative agreement with the data. Also, we have restricted our studies to the case of Newtonian fluids. Effects related to non-Newtonian liquids are probably important in the industrial issue of lubrication. As an example, in a recent study of the withdrawal out of a polymer solution in the semi-dilute regime, we reported a large thickening effect due to the Weissenberg effect. More generally the studying of coating by complex liquids (emulsions, suspensions and so on) might be a rich field of research.

It is a pleasure to thank P.-G. de Gennes, J.-M. di Meglio, P. Chartier, E. Dallies, A. Koulago, V. Shkadov and M. Velarde for discussions and encouragement.

REFERENCES

BRETHERTON, F. P. 1961 The motion of long bubbles in tubes. *J. Fluid Mech.* **10**, 166–188.

CARROLL, B. J. & LUCASSEN, J. 1973 Capillarity-controlled entrainment of liquid by a thin cylindrical filament. *Chem. Engng Sci.* **28**, 23–30.

CHEN, J. D. 1986 Measuring the film thickness surrounding a bubble inside a capillary. *J. Colloid Interface Sci.* **109**, 341–349.

DERJAGUIN, B. V. 1943 On the thickness of the liquid film adhering to the walls of a vessel after emptying. *Acta Physicochim. USSR* **20**, 349–352.

EPIKHIN, V. E. & SHKADOV, V. 1978 Flows and capillary instabilities of jets interacting with the surrounding medium. *Izv. Acad. Sci. USSR Mech. Zhid Gaza* **6**, 50–59.

ESMAIL, M. N. & HUMMEL, R. L. 1975 Nonlinear theory of free coating onto a vertical surface. *AIChE J.* **21**, 958–965.

GOUCHER, F. S. & WARD, H. 1922 The thickness of liquid films formed on solid surfaces under dynamic condition. *Phil. Mag.* **44**, 1002–1014.

KOULAGO, A., QUÉRÉ, D., RYCK, A. DE & SHKADOV, V. 1995 Film entrained by a fiber quickly drawn out of a liquid bath. *Phys. Fluids* **7**, 1221–1224.

LANDAU, L. D. & LEVICH, B. 1942 Dragging of a liquid by a moving plate. *Acta Physicochim. USSR* **17**, 42–54.

LANDAU, L. D. & LIFSHITZ, E. M. 1959 *Fluid Mechanics*. Pergamon.

LYKLEMA, J., SCHOLTEN, P. C. & MYSELS, K. J. 1960 Flow in thin liquid films. *J. Phys. Chem.* **69**, 116–123.

MOREY, F. C. 1940 Thickness of a film adhering to a surface slowly withdrawn from the liquid. *J. Res. Natl Bur. Stand.* **25**, 385–393.

MYSELS, K. J. & COX, M. C. 1962 An experimental test of Frankel's law of film thickness. *J. Colloid Sci.* **17**, 136–145.

MYSELS, K. J., SHINODA, K. & FRANKEL, S. 1959 *Soap Films*. Pergamon.

QUÉRÉ, D. & ARCHER, E. 1993 The trail of the drops. *Europhys. Lett.* **24**, 761–766.

QUÉRÉ, D., MEGLIO, J. M. DI & BROCHARD-WYART, F. 1989 Making van der Waals films on fibers. *Europhys. Lett.* **10**, 335–340.

RATULOWSKI, J. & CHANG, H. C. 1990 Marangoni effects of trace impurities on the motion of long gas bubbles in capillaries. *J. Fluid Mech.* **210**, 303–328.

RYCK, A. DE & QUÉRÉ, D. 1993*a* Fibres tirées d'un bain. *C. R. Acad. Sci. Paris (II)* **316**, 1045–1050.

RYCK, A. DE & QUÉRÉ, D. 1993*b* Entraînement visco-inertiel de liquide par un fil. *C. R. Acad. Sci. Paris (II)* **317**, 891–897.

RYCK, A. DE & QUÉRÉ, D. 1994 Quick forced spreading. *Europhys. Lett.* **25**, 187–192.

RYCK, A. DE & QUÉRÉ, D. 1995 Gravity and inertia effects in plate coating. *J. Colloid Interface Sci.* (submitted).

SEDEV, R. V. & PETROV, J. G. 1992 Influence of geometry on steady dewetting kinetics. *Colloids Surfaces* **62**, 141–151.

SOROKA, A. J. & TALLMADGE, J. A. 1971 A test of the inertial theory for plate withdrawal. *AIChE J.* **17**, 505–508.

WHITE, D. A. & TALLMADGE, J. A. 1965 Theory of drag out of liquids on flat plates. *Chem. Engng Sci.* **20**, 33–37.

WHITE, D. A. & TALLMADGE, J. A. 1966 A theory of withdrawal of cylinders from liquid baths. *AIChE J.* **12**, 333–339.